Neurobiology of Aging xxx (2015) 1–9

Contents lists available at ScienceDirect

Neurobiology of Aging

journal homepage: www.elsevier.com/locate/neuaging

High incidence of adverse cerebral blood flow responses to spreading depolarization in the aged ischemic rat brain

Ákos Menyhárt, Péter Makra, Borbála É. Szepes, Orsolya M. Tóth, Péter Hertelendy, Ferenc Bari, Eszter Farkas*

Department of Medical Physics and Informatics, Faculty of Medicine, Faculty of Science and Informatics, University of Szeged, Szeged, Hungary

ARTICLE INFO

Article history:
Received 8 May 2015
Received in revised form 30 July 2015
Accepted 12 August 2015

Keywords:
Aging
Cerebral blood flow
Electrophysiology
Cerebral ischemia
Rat
Spreading depolarization

ABSTRACT

Spreading depolarizations (SDs) occur spontaneously in the brain after stroke, exacerbate ischemic injury, and thus emerge as a potential target of intervention. Aging predicts worse outcome from stroke; yet, the impact of age on SD evolution is not clear. Cerebral ischemia was induced by bilateral common carotid artery occlusion in young (8–9 weeks old, n = 8) and old (2 year olds, n = 6) anesthetized rats. Sham-operated animals of both age groups served as control (n = 12). Electrocorticogram, direct current potential, and cerebral blood flow (CBF) variations were acquired via a small craniotomy above the parietal cortex. SDs were elicited by KCl through a second craniotomy distal to the recording site. Ischemia and age delayed the recovery from SD. CBF decreased progressively during ischemia in the old animals selectively, and inverse neurovascular coupling with SD evolved in the old but not in the young ischemic group. We propose that (mal)adaptation of cerebrovascular function with aging impairs the SD-related CBF response, which is implicated in the intensified expansion of ischemic damage in the old brain.

1. Introduction

Aging emerges as a major independent risk factor for the incidence and prevalence of ischemic stroke and predicts poor patient outcomes (Chen et al., 2010; Liu and McCullough, 2012). Considering our aging population, it is becoming ever more urgent to identify targets for therapeutic intervention to restrain the evolution of ischemic brain injury and improve stroke outcome. Much of the primary damage in the acute phase of ischemic stroke may prove irreversible despite prompt intervention, yet the management of secondary pathophysiological processes is more feasible and of fundamental importance to improve the prospect of successful recovery.

Recurrent spreading depolarizations (SDs) spontaneously occur in the cerebral cortex for at least over a week after the surgical intervention for the alleviation of primary injury in subarachnoid hemorrhage, malignant stroke, and traumatic brain injury patients (Dohmen et al., 2008; Dreier et al., 2006; Hartings et al., 2009). Moreover, SD has been recognized to contribute to the progression of delayed ischemic neurological deficit, and it has become increasingly clear that the occurrence of SD predicts worse clinical outcome from neurological casualties (Dreier et al., 2006; Hartings et al., 2011). SD, therefore, emerges as an important secondary pathogenic phenomenon in the injured brain as it has a considerable impact on lesion progression and may become a target of therapeutic strategies.

SD is a wave of intense depolarization that propagates across the cerebral gray matter and is typically followed by local changes in cerebral blood flow (CBF). The characteristic features of SD are a large, transient negative shift in the slow electrical potential (direct current potential), and the simultaneous silencing of brain electrical activity (Hartings et al., 2009; Leão, 1944; Strong et al., 2002). At the level of the nervous tissue, SD is a self-igniting cellular ionic imbalance of a critical mass of neurons and glia cells, which propagates across the gray matter at a rate of 2–6 mm/min (Somjen, 2001). When neurovascular coupling is intact, SD is associated with a CBF response containing an obvious functional hyperemic element (Hansen et al., 1980). Conversely, when neurovascular coupling is compromised (e.g., by ischemia), the SD-related hemodynamic response becomes atypical, shifting to dominant vasoconstriction (Dreier et al., 1998). This atypical CBF variation during ischemia is believed to aggravate metabolic supply-demand mismatch in the tissue (Dreier, 2011; Hoffmann and Ayata, 2013) and is thought to mediate the SD-related expansion of ischemic brain injury.

* Corresponding author at: Department of Medical Physics and Informatics, Faculty of Medicine, Faculty of Science and Informatics, University of Szeged, H-6720 Szeged, Korányi fasor 9. Hungary. Tel.: +36 62 545 829; fax: +36 62 545 077.
E-mail address: farkas.eszter.1@med.u-szeged.hu (E. Farkas).

0197-4580/$ – see front matter © 2015 Elsevier Inc. All rights reserved.
http://dx.doi.org/10.1016/j.neurobiolaging.2015.08.014

Aging was associated with the increased conversion of penumbra into infarction in patients (Ay et al., 2005), more severe ischemia-related neurological impairment in old mice, (Liu et al., 2009), and accelerated infarct development and neuronal degeneration in old rats (Popa-Wagner et al., 2007). Although SD may be implicated in all these events, the impact of aging on SD evolution, and the potential role SD might play in the age-related worsening of stroke outcome, have remained largely unexplored (Farkas and Bari, 2014).

Our group has recently made an important discovery that prolonged SDs and associated hypoperfusion likely compromise cortical tissue exposed to focal ischemia in aged rats (Clark et al., 2014). Following up on our previous work, here, we set out to determine the impact of age on the evolution of SD and the kinetics of the associated changes in local CBF in the intact and ischemic rat brain. We introduce an experimental model in which the degree of cerebral ischemia is highly reproducible, and SDs can be elicited in a planned, controlled fashion. These conditions enable the accurate evaluation of how SD evolves in the old ischemic rat brain with respect to young control.

As an addition, we introduce a detailed analysis of the electrocorticogram (ECoG) to identify specific frequency bands that may be selectively affected by SD, and to test whether spectral analysis of the ECoG can be used as a predictor for SD causing worse recovery from ischemia.

2. Materials and methods

2.1. Surgical procedures

Experimental procedures were performed with the approval of the National Scientific Ethical Committee on Animal Experimentation (updated Law and Regulations on Animal Protection: 40/2013. (II. 14.) Government of Hungary), following the EU Directive 2010/63/EU on the protection of animals used for scientific purposes.

Adult, male Sprague-Dawley or Wistar rats of 2 age groups (2 month olds, and 2 year olds, n = 26) were anesthetized with halothane or isoflurane (1.5%–2.2%, in N_2O:O_2/2:1) and allowed to breathe spontaneously through a head mask. Body temperature was kept between 37.1 °C and 37.3 °C using a heating pad, feedback-controlled by a flexible rectal probe (Homeothermic Blanket System, Harvard Apparatus, Holliston, USA). The left femoral artery was cannulated for the continuous monitoring of mean arterial blood pressure (MABP; RX104A, TSD104A, Biopac Systems, Inc, Goleta, USA). Both common carotid arteries were exposed through a ventral cervical incision. A silicone-coated fishing line used as occluder was looped around each artery for later induction of acute, incomplete, global forebrain ischemia. Animals were placed into a stereotactic frame, and 2 craniotomies were prepared on the right parietal bone (−3 mm caudal −5 mm lateral and −7 mm caudal −5 mm lateral from bregma) with a high precision dental drill (Technobox 810, Bien-Air Dental SA, Bienne, Switzerland). The dura in each craniotomy was carefully incised, and the craniotomies were regularly irrigated with physiological saline.

2.2. Ischemia induction and SD elicitation

Ischemia induction was preceded by a 10-minute baseline period, during which all variables were continuously recorded. Acute global forebrain ischemia was induced by pulling on the occluder lines looped around the common carotid arteries and securing them in place (“two-vessel occlusion”, 2VO) in a young and in an old group of rats (young 2VO, n = 8; and old 2VO, n = 6). In an age-matched young group used as control for the surgical procedures, the occluders were in place but not pulled on (young control, n = 6). For the old age-matched control group, acute 2VO was not implemented either; instead, animals had undergone permanent 2VO produced 1-year prior SD elicitation (old control, n = 6).

Recurrent SDs in all groups were triggered by placing a 1M KCl-soaked cotton ball on the exposed cortical surface in the caudal cranial window 10 minutes after 2VO onset. In old rats, 1M KCl often proved insufficient to trigger SD, therefore, either 3M KCl was used, or—if still inefficient—a tiny KCl crystal was placed on the cortical surface to achieve SD elicitation. Experiments were terminated by the overdose of the anesthetic agent.

2.3. Electrophysiology

In the rostral craniotomy, slow cortical or direct current (DC) potential and ECoG were acquired through a glass capillary electrode (20 μm outside tip diameter) filled with saline, implanted 1–1.2 mm deep into the cerebral cortex. An Ag/AgCl reference electrode was placed subcutaneously in the neck. DC potential and ECoG were recorded via a high-input impedance preamplifier (NL102G, NeuroLog System, Digitimer Ltd Welwyn Garden City, Hertfordshire, England), connected to a differential amplifier (NL106, NeuroLog System, Digitimer Ltd) with associated filter and conditioner system (NL125, NL530,Digitimer Ltd, NeuroLog System). Potential line frequency noise (50 Hz) was removed by a high-quality noise eliminator (HumBug, Quest Scientific Instruments Inc, North Vancouver, Canada) without any signal attenuation. Signals were acquired at a sampling frequency of 1 kHz. Analog to digital conversion was performed by a dedicated data acquisition system (MP 150, Biopac Systems, Inc).

Data analysis was assisted by the inbuilt instructions of the software AcqKnowledge 4.2 for MP 150 (Biopac Systems, Inc). For each SD, the amplitudes of depolarization and hyperpolarization were defined as the maximum of the negative and positive shift relative to baseline in DC potential, respectively and were expressed in mV. The maximum rates of depolarization and repolarization were calculated as the respective slopes of the SD-related DC shift given in mV/s. The duration of SD events was measured at half amplitude of the SD-related negative DC shift in seconds.

2.4. Monitoring of local CBF

SD-associated changes in local CBF adjacent to the glass capillary electrode were recorded by using laser-Doppler flowmetry (LDF). A stainless steel needle Doppler probe (Probe 403, connected to Periflux 5000, Perimed UK Ltd, Bury St Edmunds, UK) was positioned at an angle with a micromanipulator close to the penetration point of the glass capillary electrode. Care was taken to avoid large pial vessels. The LDF signal was digitized together with the DC potential and ECoG as described previously (MP 150, Biopac Systems, Inc).

All variables (i.e., DC potential, ECoG, LDF signal, and MABP) were simultaneously acquired, displayed live, and stored using a personal computer equipped with a dedicated software (AcqKnowledge 4.2 for MP 150, Biopac Systems, Inc).

Six types of hemodynamic responses were identified, ranging from dominating hyperemia to prolonged cortical spreading ischemia with intermediate forms. The CBF response to each SD was classified accordingly, and the prevalence of various CBF response types was determined for each experimental group.

SD-associated relative changes in local CBF were calculated based on 100% baseline taken shortly before SD occurrence and residual LDF signal after anesthetic overdose considered as biological zero. The magnitude of each element of the SD-related CBF

response (i.e., initial hypoperfusion, transient hyperemia, prolonged oligemia) was expressed relative to baseline (%). The duration of early hypoperfusion and subsequent transient hyperemia was measured at half amplitude of the initial hypoemic drop and hyperemic peak.

2.5. Spectral analysis of ECoGs

The analysis was carried out to reveal whether the dynamics of SD-related electrical silence of neural activity is selective for specific frequency ranges, and what impact ischemia might exert on these parameters. Only the young control and young 2VO groups were included in the analysis because the ECoG of the old animals was excessively noisy. The 4 conventional frequency ranges (i.e., alpha: 8–13 Hz; beta: 13–30 Hz; delta: 0.5–3 Hz; and theta: 3–8 Hz) that covered the full spectrum up to 30 Hz (the effective edge of low-pass filtering of the ECoG) were treated separately. All spectral calculations were carried out in a self-developed .NET environment written in C#. Fast Fourier transforms were calculated using a .NET wrapper around FFTW (the Fastest Fourier Transform in the West, http://www.fftw.org/). The Task Parallel Library offered by .NET was also used to speed up calculations.

The basis of the spectral investigations is the short-time Fourier transform (STFT) of the relevant ECoG sequence $\{\varepsilon_k\}_{k=0}^{N-1}$. Advancing a Gaussian window w_k of width $W\Delta t = 60$ s (wherein $\Delta t = 0.001$ s denotes the sampling interval) along the ECoG sequence in steps of $\Delta\tau = 1$s, one can obtain the STFT value at time $t_m = m\Delta\tau$ and frequency $f_n = n\Delta f = \frac{n}{W\Delta t}$ as

$$E(t_m, f_n) = E_{m,n} = \sum_{k=0}^{W-1} w_k \varepsilon_{m+k} e^{-i\frac{2\pi}{W}kn}$$

From the STFT, a time-dependent power spectral density $S(t_m, f_n)$ can be calculated as follows:

$$S(t_m, f_n) = S_{m,n} = \frac{|E_{m,n}|^2 \Delta t}{W}$$

The integrated spectral power $P(t_m) = P_m$ of a given frequency range between $f_{\min} = n_{\min}\Delta f$ and $f_{\max} = n_{\max}\Delta f$ is the integral of the power spectral density between these limits, which, in discrete representation can be calculated as

$$P(t_m) = P_m = \sum_{n=n_{\min}}^{n_{\max}-1} S_{m,n}\Delta f = \sum_{n=n_{\min}}^{n_{\max}-1} \frac{|E_{m,n}|^2 \Delta t}{W} \cdot \frac{1}{W\Delta t} = \sum_{n=n_{\min}}^{n_{\max}-1} \frac{|E_{m,n}|^2}{W^2}$$

The integrated spectral powers follow a trench-like profile during an SD episode. These trench profiles were modeled as a series of straight-line segments. The 4 breakpoints bounding the downward and upward segments were marked manually, then a parallel search was carried out in the neighborhood of these initial breakpoints to find the positions for which the least-squares fit of these segments provides the least residual sum of squares. The baseline (first) and recovery (last) segments were always horizontal and 60 seconds long, representing the mean spectral power before and after the SD, respectively. Finally, to produce a contiguous segment sequence, each segment was extended or reduced to the point where it intersects the neighboring segment. The parameters obtained from the trench profiles were the following: ① level of baseline (the mean spectral power for the 60-second interval preceding the onset of an SD); ② slope of depression (the slope of the downward segment); ③ level of depression (the arithmetic mean between the endpoints of the downward and upward segments); ④ duration of depression (expressed in seconds); ⑤ slope of recovery (the slope of the upward segment); ⑥ level of recovery (the mean spectral power for the 60-second interval following recovery).

Alpha-to-delta ratio (ADR) has been reported to represent neural activity: lower values were taken as a predictor of worse recovery from ischemia in patients (Claassen et al., 2004). Therefore, ADR values were calculated for the 3 horizontal segments (i.e., baseline, depression, and recovery) as simply the ratio of the integrated power of the alpha range to that of the delta range:

$$\mathrm{ADR}_s = \frac{P_{\alpha,s}}{P_{\delta,s}},$$

wherein, the index s indicates the segment for which the ADR is calculated (baseline, depression, or recovery), and P stands for the integrated alpha or delta power for the given segment (e.g., $P_{\alpha,1}$ is the level of baseline for the alpha trench profile while $P_{\delta,3}$ denotes the level of recovery in the delta trench profile).

2.6. Statistical analysis

Data are given as mean ± standard deviation for parametric data, and median (interquartile range 95%) for nonparametric data. The software SPSS (IBM SPSS Statistics for Windows, Version 20.0. Armonk, NY: IBM Corp) was used for statistical analysis. A one-way analysis of variance (ANOVA) paradigm followed by a Fisher post hoc test was applied for the evaluation of data derived from the DC potential, and the duration of transient hyperemia. The prevalence of CBF response types across experimental groups was evaluated with the nonparametric Fisher's exact test. The magnitude of the elements of the CBF response, the SD-related changes in the integrated power of the 4 frequency ranges of the ECoG, and the temporal changes in ADR were tested with repeated measures ANOVA. Data obtained by the spectral analysis of ECoG were tested by a multivariate ANOVA paradigm, followed by a Fisher post hoc test. Correlation analysis between the duration of the SD-related negative shift in DC potential and transient hyperemia was performed with Spearman correlation analysis. Level of confidence was given as $^{*}p < 0.05$ and $^{**}p < 0.01$.

3. Results

3.1. Mean arterial blood pressure and CBF variations in the ischemia model used

Baseline MABP values were similar across all groups (95 ± 3.6 mm Hg), followed by a slight, 4 ± 11.5 mm Hg increase above baseline during ischemia, and a small reduction of 4 ± 8.6 mm Hg below baseline after reperfusion initiation in the ischemic groups, with no age-related statistical difference.

Ischemia induction by 2VO caused a marked drop of CBF in the young 2VO and old 2VO groups to 41 ± 9.4% and 38 ± 18.2% of baseline, respectively. In contrast, CBF taken at the end of the ischemic period persisted at 43 ± 22.1% in the young 2VO group, but decreased further to 18 ± 13.6% in the old 2VO group, being significantly lower than CBF in the same group earlier at ischemia onset ($p < 0.024$), or CBF in the young 2VO group at the end of ischemia ($p < 0.028$). Finally, CBF peaked during reperfusion at 83 ± 27.6% and 106 ± 62.1% in the young 2VO and old 2VO groups, respectively, with no statistically significant difference due to age ($p < 0.366$). No CBF variation was observed throughout the experimental period in the control groups.

3.2. The DC potential signature of SD

The approach of SD elicitation (i.e., placing a KCl-soaked cotton ball on the exposed cortical surface) induced recurrent SDs at irregular intervals. In the young groups, SD elicitation with the topical application of 1M KCl was successful in each experiment; by contrast, 1M concentration of KCl was insufficient to trigger SD in the old groups—instead, 3M KCl or, when still ineffective, a small KCl crystal was required for SD generation, indicative of a higher elicitation threshold for SD in the old animals.

SDs were transient (i.e., transient negative shifts in the DC potential, Fig. 1A), except for 1 animal in the old 2VO group, in which the first SD appeared to be terminal (i.e., no recovery of the DC potential, synchronous with a constant isoelectric ECoG signal till the termination of the experiment). In general, 2–3 SDs were recorded in the young 2VO and old 2VO groups during ischemia, in contrast with 4–5 SDs in the respective nonischemic control groups, showing a tendency for lower SD frequency during ischemia.

Because recurrent SDs occurred at irregular intervals, often in a rapid succession that disabled the reliable analysis of the CBF responses associated with subsequent SDs, the first SD alone was analyzed comprehensively. As Fig. 1A demonstrates, the most obvious effect of ischemia was the elongated duration of the SD-related negative DC shift (e.g., 66.2 ± 22.8 vs. 21.4 ± 4.1 seconds, young 2VO vs. young control; Fig. 1B), which was augmented further by age as seen in the old 2VO group (95.8 ± 46.2 seconds, Fig. 1B). The ischemia-related, elongated duration of SDs was also reflected in the reduced slopes of depolarization (14.5 ± 11.4 vs. 4.4 ± 2.9 mV/s, young 2VO vs. young control; Fig. 1 C) and repolarization (0.7 ± 0.5 vs. 2.6 ± 0.7 mV/s, young 2VO vs. young control; Fig. 1D). Old age was associated with a reduced slope of depolarization, as well (1.9 ± 0.9 vs. 2.6 ± 0.7 mV/s, old control vs. young control; Fig. 1C). Finally, the amplitude of depolarization and repolarization tended to be smaller in the ischemic groups (Fig. 1E and F), and older age was associated with a reduced amplitude of repolarization (2.9 ± 2.9 vs. 5.1 ± 1.2 mV, old control vs. young control; Fig. 1F).

3.3. Laser-Doppler recording of CBF response to SD

First, screening all experimental groups and all SDs elicited, 6 types of SD-associated CBF response were determined based on the kinetics of their laser-Doppler trace. As shown in Fig. 2A, the CBF response types were ranked from the physiological types (type 1 and type 2) toward those consisting of a decreasing hyperemic and more obvious hypoemic component (types 3–5), ending with spreading ischemia (type 6). In addition, a few SDs occurred without a detectable variation in CBF (i.e., no CBF response). Because the most important parameter in the spectrum from normal hyperemic responses to inverse responses is the increasing duration of the initial hypoperfusion (Dreier et al., 2001; Hoffmann and Ayata, 2013), its duration was quantified (table in Fig. 2A). As expected, early hypoperfusion was increasingly more represented with higher rank CBF response types.

Next, the distribution of the defined CBF response types associated with the first SD was evaluated across experimental groups (Fig. 2B). The young control group displayed only the physiological type 1 (n = 4/6) and type 2 (n = 2/6) responses, while the first SD in the young 2VO animals was coupled with types 3–5 response, type 4 being the most frequent of all (n = 5/8). The old control group

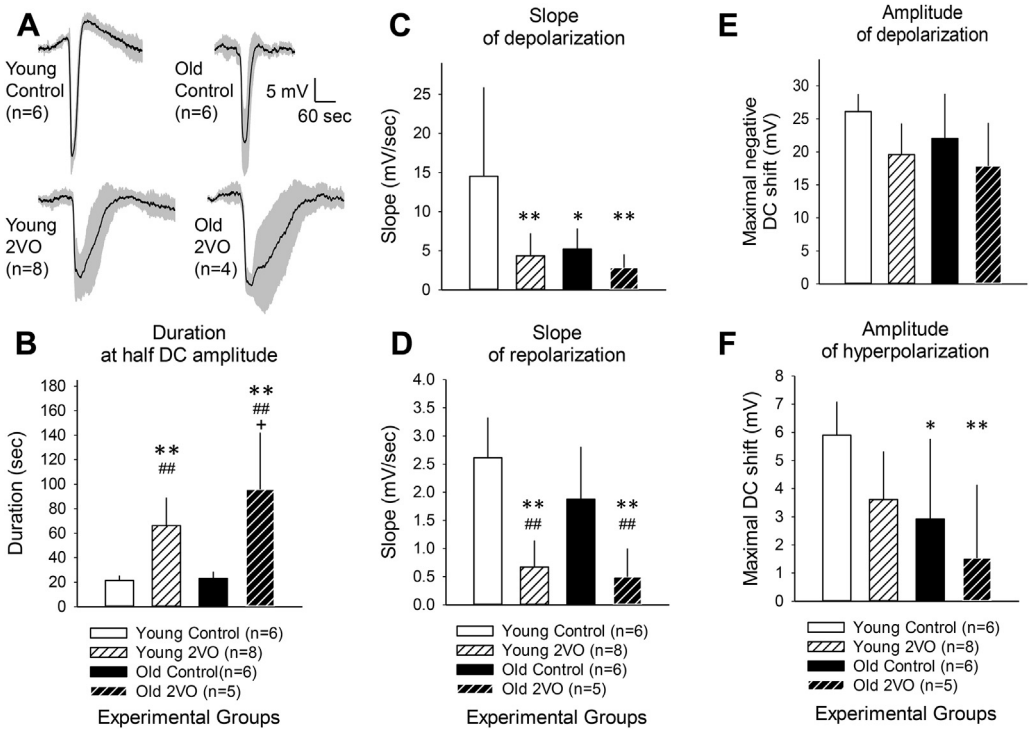

Fig. 1. Age- and ischemia-related changes in the direct current (DC) potential signature of first evoked spreading depolarization (SD1) in each experiment. (A) Traces of SD-related negative DC shifts (mean ± standard deviation) for each experimental group; (B) duration of SD measured at half amplitude of the negative DC shifts; (C) maximum rate of depolarization determined as the slope of the negative DC shift; (D) maximum rate of repolarization calculated as the slope of the positive DC shift. (E) Amplitude of the SD-related depolarization given as the maximum negative DC shift with respect to baseline; (F) amplitude of the SD-related hyperpolarization measured as the maximum positive DC shift during repolarization with respect to baseline; all data are given as mean ± standard deviation. A one-way ANOVA (analysis of variance) paradigm followed by a Fisher post hoc test was applied for statistical analysis. Levels of significance are given as $^{*}p < 0.05$, $^{**}p < 0.01$ versus young control, $\#\#p < 0.01$ versus old control, $+p < 0.05$ versus young 2VO. Abbreviations: control, sham-operated control; 2VO, 2-vessel occlusion (bilateral common carotid artery occlusion).

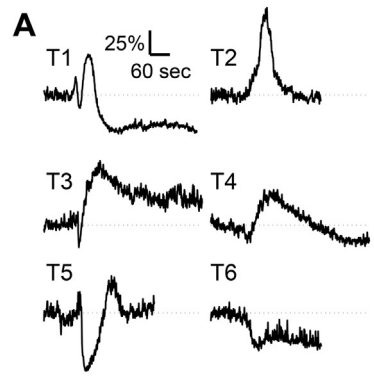

Type	Duration of early hypoperfusion (s, mean±stdev)
1	9.09±6.4
2	n.a.
3	7.87±7.2
4	25.82±20.5
5	48.51±18.8
6	2010±226**

One-way ANOVA: F=323.091**

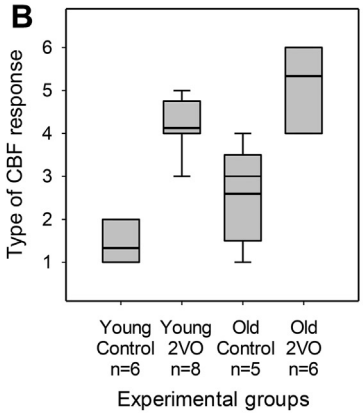

Group	Duration of early hypoperfusion (s, mean±stdev)
Young Control	7.9±6.8
Young 2VO	36.8±17.5
Old Control	4.6±5.2
Old 2VO	1344±1047**

One-way ANOVA: F=10.855**

Fig. 2. Various kinetics of the spreading depolarization (SD)-related cerebral blood flow (CBF) response. (A) Types of detectable CBF response associated with SD events. Each type is demonstrated by a representative trace. CBF responses were ranked from the physiological types toward those consisting of a decreasing hyperemic and more obvious hypoemic component. The table in panel A displays the mean duration of early hypoperfusion (i.e., hypoemic component) for each type, to indicate the progressively increasing share of hypoperfusion in the full CBF response (**$p < 0.001$, type 6 vs. type 1). (B) Distribution of the defined types of CBF response across experimental groups. The box plot displays data for the first SD (SD1). Data were evaluated with the nonparametric Fisher's exact test. Level of confidence was determined as **$p < 0.001$. The table in panel B shows the mean duration of early hypoperfusion (i.e., hypoemic component) for each experimental group (**$p < 0.001$, old 2VO vs. all other groups). Abbreviations: ANOVA, analysis of variance; CBF, cerebral blood flow; control, sham-operated control, stdev, standard deviation; 2VO, 2-vessel occlusion (bilateral common carotid artery occlusion).

developed a wide spectrum of CBF responses ranging between types 1–4, including an animal with no CBF response, which displayed an age-related shift to higher rank types as compared with the young control group. The first SDs in the old 2VO group were associated with either type 4 (n = 2/6) or type 6 (n = 4/6) CBF response, showing a striking share of spreading ischemia (i.e., type 6). Quantitative analysis of the duration of early hypoperfusion (table in Fig. 2B) indicated that this first element of the CBF response to SD was elongated during ischemia (36.8 ± 17.5 vs. 7.9 ± 6.8 seconds, young 2VO vs. young control) and became drastically longer in the old 2VO group (1344 ± 1047 seconds), due to the prevalence of spreading ischemia.

The quantitative analysis (Fig. 3) relying on the hyperemic type 1–5 CBF responses (i.e., those containing a transient hyperemic element) revealed that ischemia reduced the amplitude of hyperemia in both young (57 ± 10.1 vs. 156 ± 47.7%, young 2VO vs. young control) and old animals (30 ± 17.9 vs. 181 ± 72.7%, old 2VO vs. old control). At the same time, ischemia extended the duration of hyperemia significantly (237 ± 97 vs. 37 ± 12 seconds, young 2VO vs. young control; 122 ± 75 vs. 46 ± 14, old 2VO vs. old control). Taken together, the hyperemic CBF responses to SDs were of smaller amplitude but longer duration under ischemia.

Finally, potential association between the duration of the first SD-related negative DC shift and transient hyperemia was tested as shown in Fig. 3D, which revealed a very strong correlation (R = 0.824) between the two variables.

3.4. Spectral analysis of ECoGs

Taken the trench profile of the integrated power for each ECoG frequency range, the delta and theta ranges appeared to be dominating, while the alpha and delta ranges represented a significantly lower share in the ECoG during baseline and recovery (Fig. 4A).

The rank of SD (i.e., first or second) had a marked impact on the level of depression, which was almost twice as high for SD2 than for SD1, irrespective of ischemia (Fig. 4B). On the other hand, the duration of ECoG depression doubled during ischemic SDs as compared with the nonischemic time controls for the alpha (152 ± 70 vs. 73 ± 42 seconds), delta (160 ± 88 vs. 87 ± 65 seconds) and theta (146 ± 82 vs. 78 ± 50 seconds) frequency ranges (Fig. 4D). Correspondingly, the slope of recovery during ischemic SDs was only half of the nonischemic time-control events in all frequency ranges (Fig. 4C). Finally, ADR was substantially higher during depression as compared with baseline and recovery, with no impact of SD rank or ischemia (Fig. 4E).

4. Discussion

4.1. Advantages and limitations of the experimental approach

Experimental studies that set ischemic SDs as their target of investigation predominantly rely on focal ischemia models, in which recurrent SDs occur spontaneously; yet, the systematic analysis of spontaneous SDs remains challenging (Bere et al., 2014b). Even widely accepted ischemia models, such as middle cerebral artery occlusion are known to produce quite some variation in ischemia severity (Duverger and MacKenzie, 1988)— probably because of the anatomic variation in middle cerebral artery branching patterns (Fox et al., 1993; Rubino and Young, 1988)— which, in turn, will cause variations in the site of SD elicitation, direction of SD propagation, SD type (i.e., short transient or prolonged), and SD pattern (i.e., single events or clusters). A further, inherent limitation of this approach is that nonischemic time control cannot be implemented due to the unpredictable occurrence of spontaneous SDs. For these reasons, we imposed 2VO, which produces an immediate, reproducible drop in CBF without the successive occurrence of spontaneous SDs in adult Sprague-Dawley rats (Bere et al., 2014a), allowing (1) planned, controlled SD elicitation during ischemia by the topical application of KCl, and (2) the design of nonischemic time control experiments.

Despite these major advantages of the model, some shortcomings have emerged during the progression of the study. First, the elicitation of SDs by continuous exposure of the brain surface to KCl (Farkas et al., 2011) produced SDs at a rather high frequency, which hampered the latter analysis of all SDs triggered, leaving the first 1–2 SDs to be evaluated reliably. Second, the unexpected condition that 1M KCl will not generate SDs in 2-year-old rats, together with the necessity to produce SDs to assess age-related features of SD evolution prompted us to use higher concentration KCl for SD induction in old rats. This led us to conclude that the SD threshold must be significantly higher in the aged brain (consistent with previous observation on brain slices) (Maslarova et al., 2011) but did not allow the precise quantification of SD threshold. We resolved both of these issues in a subsequent study of ours.

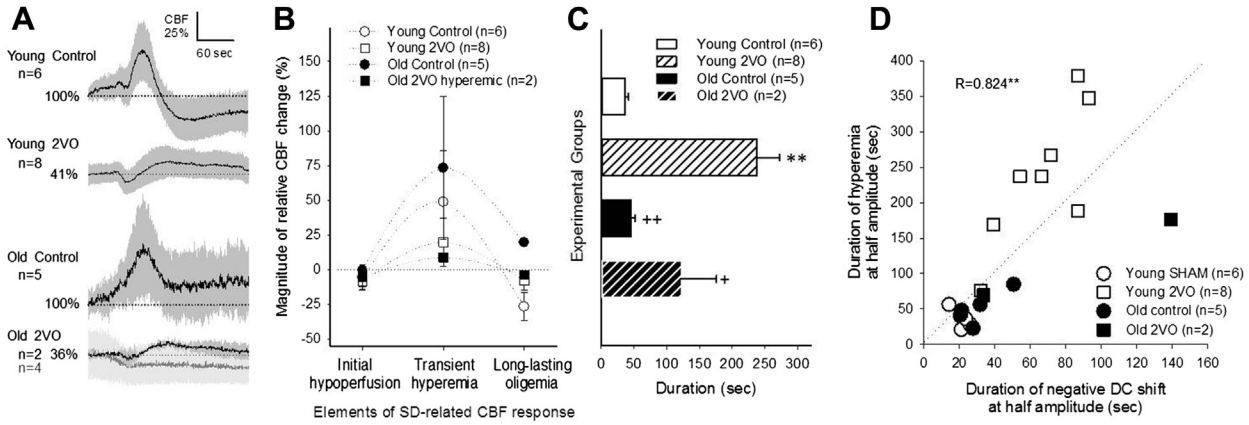

Fig. 3. Quantitative evaluation of the cerebral blood flow (CBF) response coupled with the first spreading depolarization (SD) event in each experiment. (A) Average CBF response (mean ± standard deviation) illustrated for each experimental group. Horizontal dotted lines indicate mean CBF (%) prior SD elicitation. In the old 2VO group, hypoemic CBF response was detected in 4 of 6 animals (gray trace). (B) Magnitude of the 3 distinct elements of the SD-associated CBF response (mean ± standard deviation). Repeated measures analysis of variance (ANOVA) was used for statistical analysis (group effect: $^{**}p < 0.003$). A Fisher post hoc test revealed a significant difference in the kinetics of the CBF response in the young 2VO and old 2VO groups with respect to the young control group ($^{**}p < 0.002$). The difference between the old control and old 2VO groups was also nearly significant ($p < 0.057$). (C) Duration of transient hyperemia (mean ± standard deviation). A one-way ANOVA paradigm followed by a Fisher post hoc test was applied for statistical analysis. Levels of confidence were determined as $^{**}p < 0.001$ versus young control, $+p < 0.05$ and $++p < 0.001$ versus young 2VO. (D) Correlation between the duration of the SD-related negative DC shift and the hyperemic element of the associated CBF response for the first SD event. Statistical evaluation relied on Spearman correlation analysis. Abbreviations: control, sham-operated control; 2VO, 2-vessel occlusion (bilateral common carotid artery occlusion).

Finally, the study was conducted with the use of 2 distinct anesthetic agents and mixed strains of rats due to uncontrollable external conditions. Still, the acquired data are highly consistent with our previous findings obtained with the use of halothane-anesthetized Wistar rats (Clark et al., 2014). Furthermore, we carefully considered any potential impact of the type of anesthesia on all the read-outs presented, by including the type of anesthesia as a factor into the statistical analysis. This approach excluded the

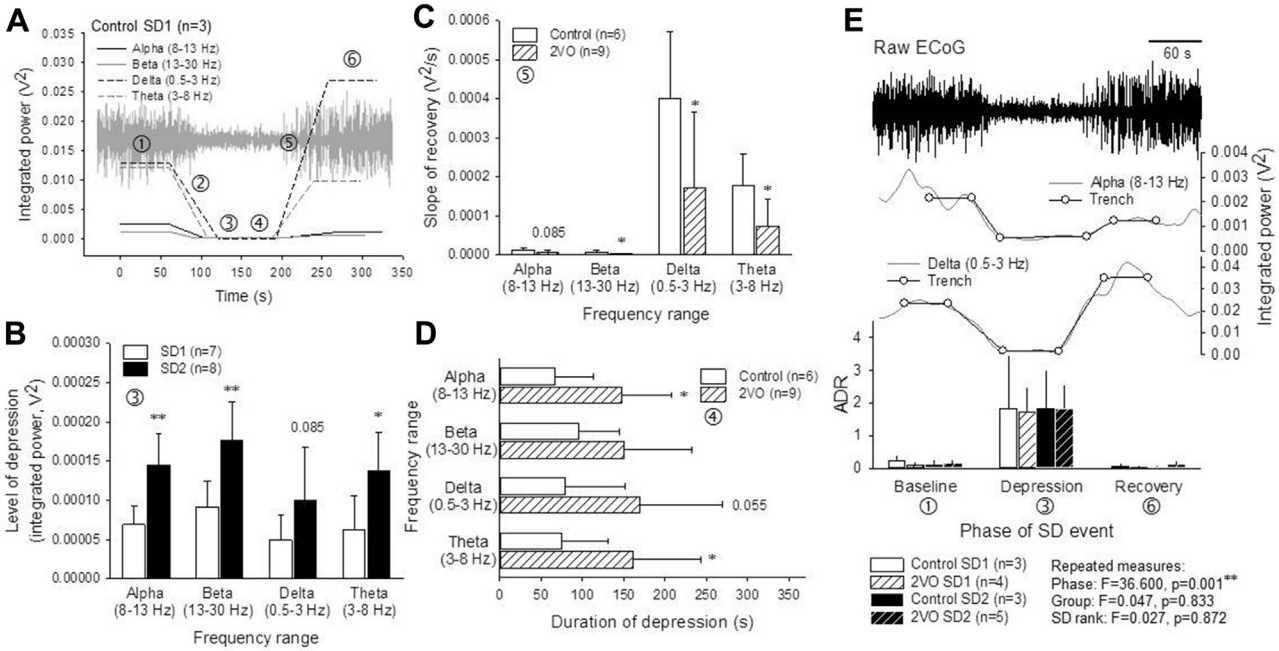

Fig. 4. Analysis of spreading depolarization (SD)-associated changes in spectral powers of the electrocorticogram (ECoG). Six individual ECoG parameters were evaluated based on the computation of integrated power for the 4 established ECoG frequency bands (i.e., alpha: 8–13 Hz, beta: 13–30 Hz, delta: 0.5–3 Hz, and theta: 3–8 Hz): level of baseline (①), slope of depression (②), level of depression (③), duration of depression (④), slope of recovery (⑤), and level of recovery (⑥). (A) Trench profiles determined by the time dependence of the spectral powers for each of the 4 frequency ranges are shown. Each line representing a given frequency range was obtained by taking the mean value for SD1 of 3 young control animals. In the background, an original, representative ECoG trace taken during SD1 of a young control animal is shown in gray. (B) Bar charts demonstrate the level of depression during SD1 and SD2 for each frequency range of the ECoG. (C) The slope of recovery is displayed for the young control and 2VO groups for each frequency range of the ECoG. (D) The duration of depression is shown for the young control and 2VO groups for each frequency range of the ECoG. (E) Alpha-to-delta ratio (ADR) was calculated for the 3 phases (i.e., baseline, depression, recovery) of the SD-related ECoG signal. Below a representative, original ECoG trace during SD, the derived integrated power plots and related trench profiles for the alpha and delta frequency ranges are presented. The bar chart at the bottom shows ADR values for the young control and 2VO groups, with SD1 and SD2 assessed apart. Each bar in the charts represents mean ± standard deviation. A multivariate analysis of variance paradigm followed by a Fisher post hoc test was used for the statistical evaluation of data in panels B, C, and D. A repeated measures analysis approach was applied for the statistical analysis of the data in panel E. Level of significance was determined as $^{*}p < 0.05$ and $^{**}p < 0.01$. Abbreviations: control, sham-operated control; 2VO, 2-vessel occlusion (bilateral common carotid artery occlusion).

possibility that halothane and isoflurane affected MABP, the DC potential signature of SD or CBF differently. We did find, however, an anesthesia-related effect on the variables obtained from spectrum analysis of the ECoG (i.e., isoflurane systematically reduced the slope and level of recovery after SD, and elevated ADR, as compared with halothane), therefore only halothane-anesthetized rats (n = 15) were included in the final quantitative analysis of the ECoG data.

4.2. The recovery of resting membrane potential after depolarization is delayed during ischemia and in old age

We have shown here that SD duration at half DC amplitude and ECoG depression become significantly longer during ischemia, together with a considerable reduction in the slopes of depolarization and repolarization and the recovery of activity as seen on the ECoG. It has been generally accepted that as the same SD propagates from ischemic to nonischemic cortex, its duration progressively decreases toward the nonischemic tissue (Nedergaard, 1996; Shin et al., 2006).

In the present study, the longer duration of SD in the ischemic brain is attributed to the collective, lower rate of depolarization and repolarization, rather than the prolongation of complete depolarization itself (Bere et al., 2014a). During the depolarization phase of SD, there is an intense efflux of K^+ to the extracellular space, parallel with considerable influx of Na^+ (Hansen and Zeuthen, 1981; Somjen, 2001). In ischemia, the concentration gradient between the intracellular and extracellular compartments becomes lower than in physiological brain tissue (i.e., $[Na^+]_e$, decreases from 140 to 80 mM, $[K^+]_e$ increases from 5 to 20–60 mM, with parallel but opposite changes in intracellular ion composition) (Dugan and Choi, 1999; Rossi et al., 2007). This results in a considerably reduced (but still substantial) transmembrane ionic concentration gradient during SD in the ischemic brain tissue (Somjen, 2001). Therefore, the driving force for K^+ efflux and Na^+ influx that take place during the depolarization phase of SD may decrease, which is thought to be reflected in the lower rate of depolarization as measured here.

The optimal function of Na^+/K^+–adenosine triphosphatase (ATPase) is essential for the restoration of membrane potential following SD. During ischemia, oxidative substrate supply declines, and tissue ATP availability decreases, which lead to the reduction of Na^+/K^+-ATPase activity (Dreier, 2011), thereby potentially delaying the restoration of transmembrane potential.

Old-age aggravated the ischemia-related prolongation of SD duration: 1 of the 6 animals in the old 2VO group displayed terminal depolarization, and the duration of transient first SDs was significantly longer as compared with the young 2VO group. These results stand in agreement with our previous observation made in a focal forebrain ischemia model that the cortical surface involved in prolonged SDs was significantly larger in old as compared with young rats (Clark et al., 2014). These data together indicate that the aged ischemic brain has scarcer resources to recover from an SD event, which reflects the increased vulnerability of the aged brain to ischemia- and/or SD-related injury.

Finally, the DC potential signature of SDs revealed that the amplitude of hyperpolarization in old rats was approximately half of their young counterparts. Hyperpolarization after SD appears to be a transient overshoot of either $[Na^+]_e$ due to the increased activity of Na^+/K^+ ATPase, or $[Cl^-]_e$ (Hansen and Zeuthen, 1981). Aging may have an impact on either of these ion fluxes; yet it remains uncertain which exact mechanism(s) must be responsible for the age-related reduction in the amplitude of hyperpolarization seen in our study.

4.3. The hyperemic response to SD diminishes during ischemia and becomes inverted in the aged ischemic brain

The SD-coupled CBF response in the physiologically intact rat cortex consists of at least 3 distinct elements: an initial transient vasoconstriction, a marked hyperemia, and a long-lasting oligemic phase (Ayata, 2013). Ischemia shifts this balance toward the domination of the initial vasoconstrictive (hypoemic) element of the pattern, possibly as a function of decreasing perfusion pressure (Bere et al., 2014b; Hoffmann and Ayata, 2013). Matching this concept, we have identified 6 types of CBF kinetics ranging from dominating hyperemia to prolonged cortical spreading ischemia with intermediate forms. The types observed during ischemia have, coincidentally, a perfect match with those described earlier in the ischemic cortex of stroke patients (Woitzik et al., 2013).

Major observations of the presented research are as follows: (1) the SD-coupled CBF response types, in which the hypoemic component is augmented at the expense of the hyperemic component, occur more frequently in the aged brain, (2) the combination of ischemia and old age predisposes the cortex for the evolution of spreading ischemia (inverse neurovascular coupling), and (3) the ischemia-related perfusion deficit progressively deepens in the old brain as opposed to the young. During physiological aging, unfavorable changes occur in the brain's microcirculation, including increased vascular wall stiffness (Farkas and Luiten, 2001), decreased vascular density (Faber et al., 2011), impaired microvascular reactivity (Park et al., 2007), and weakened remodeling potential (Faber et al., 2011). The additive outcome is lower basal CBF, but more importantly, reduced, suboptimal local CBF elevation in response to neural activity, which is suggested to contribute to the shift to less obvious hyperemic and more prominent hypoemic elements in the SD-associated CBF response.

The high incidence of inverse coupling in the old ischemic rats (also seen in our previous study concerning focal cerebral ischemia, Clark et al., 2014) is proposed to be determined by the combination of vasoconstrictive high $[K^+]_e$ and the restricted availability of the vasodilator nitric oxide (NO) (Windmüller et al., 2005). Ischemia itself imposes considerable extracellular K^+ accumulation above the dilation and/or constriction threshold (20 mM) (Hansen and Zeuthen, 1981), and NO is quickly eliminated by its reaction with superoxide yielding peroxynitrite (Warner et al., 2004). Limited NO availability due to increased free radical production causes dysfunctional NO-based vasodilation during physiological aging, as well (Mayhan et al., 2008; Ungvari et al., 2010). Ischemia superimposed on aging, therefore, is thought to potentiate the impairment of NO-based vasoregulation in the face of high $[K^+]_e$, which may lead to a higher incidence of inverse neurovascular coupling in the aged ischemic brain. In turn, the resultant spreading ischemia is suggested to deepen the perfusion deficit imposed by ischemia.

4.4. Perfusion deficit during ischemia deepens progressively in the aged but not in the young brain

CBF sharply drops after ischemia onset, but compensation through collaterals or vascular remodeling may contribute to slow partial recovery of perfusion (Clark et al., 2014; Lapi and Colantuoni, 2015). Our data indicate that in the ischemia model used, perfusion stabilized and persisted at around 40% till the end of the ischemic period in young rats, but dropped below 20% in old rats, which falls below the CBF threshold of electrical failure of the nervous tissue (Astrup et al., 1977). This was also confirmed by the lasting depression of ECoG during ischemia in our old rats. Although age-related cerebrovascular rarefaction may be held responsible for the poor flow compensation in aged rats (Faber et al., 2011), we believe that the ischemia-induced perfusion deficit in our study

was aggravated by the high incidence of inverse neurovascular coupling with SD in old animals. Thus, SDs associated with spreading ischemia likely impair the recovery of CBF, thereby worsening ischemia outcome.

4.5. Spectral analysis of ECoGs reveals equal involvement of all frequency bands and milder depression with recurrent SDs

The spectral analysis of the ECoG revealed at baseline and recovery that the weight of low frequency bands in the spectrum (i.e., delta and theta) is greater than that of higher-frequency waves (i.e., alpha and beta) (Fig. 4A). This mainly reflects an inherent feature of ECoG spectra: because the ECoG frequency bands represent a power spectrum, their values will vary exponentially, meaning the lower-frequency bands will have exponentially greater values than the higher-frequency bands. In addition, halothane anesthesia may also accentuate the relative weight of low frequencies, because it decreases the power of higher frequency waves (i.e., alpha and beta) (Dougherty et al., 1997).

Spectral analysis of the 4 frequency ranges was implemented to examine whether the SD-related depression of electrical activity would appear in a distinct form on the various bands of the power spectrum. During SD, all 4 frequency ranges depressed synchronously (Fig. 4A), reached the same level of depression for a given SD (Fig. 4B), and recovered after a period of depression of similar duration (a bit over a minute in the nonischemic brain, Fig. 4D). The only significant difference between the 4 waves concerned the slopes of depression and recovery (being considerably lower for the alpha and beta waves, Fig. 4C), but this may not have functional significance since the shallower slope for the higher frequencies was generated by the smaller power difference between baseline or recovery and depression (i.e., lower level of baseline or recovery but the same level of depression). In summary, SD appeared in a similar fashion on all 4 frequency ranges of the ECoG under halothane anesthesia.

The observation that the level of depression for the second SD remained higher as compared with the first SD appears to be unique. These data suggest that the electrical silence with the second SD must be incomplete. Although the difference in the kinetics of the CBF response to the first and second SD in a sequence is well-known (Obrenovitch et al., 2009), according to the best of our knowledge this is the first evidence to demonstrate variation in the level of depression with recurrent SDs.

Low ADR value has been reported to represent slow ECoG (i.e., higher share of low frequencies) and was taken as a predictor of worse recovery from delayed cerebral ischemia of subarachnoid hemorrhage patients (Claassen et al., 2004) and pentobarbital-anesthetized ischemic rats (Liao et al., 2015). Based on these accounts, together with the widely accepted notion that SD worsens ischemic brain injury (Back et al., 1996; Dreier, 2011), we set out to calculate ADR with the expectation to get lower ADR values after the passage of an SD as an indication for its injurious potential. During SD, both alpha and delta waves became depressed to a similar level, which increased the calculated ADR significantly with respect to baseline. The high ADR in this case should not be interpreted as a lower ratio of slow waves (Claassen et al., 2004; Liao et al., 2015), therefore, it can give no predictions as to functional outcome. During the phase of recovery from SD, ADR returned to baseline with no difference between ischemic and nonischemic tissue, therefore, our hypothesis that ADR following SD in the ischemic tissue would decrease to indicate worse recovery was not proven. Because the calculations could not be carried out in the old groups due to excessive noise on the ECoG recordings and spreading ischemia was detected in these old animals, it remains possible that ADR following SDs with inverse neurovascular coupling would indicate dysfunction. This possibility is to be tested in our subsequent studies.

Disclosure statement

The authors have no conflicts of interest to disclose.

Acknowledgements

This work was supported by grants from the Hungarian Scientific Research Fund (Grant No. K111923), the Hungarian Brain Research Program (Grant No. KTIA_13_NAP-A-I/13), and the Bolyai János Research Scholarship of the Hungarian Academy of Sciences (BO/00327/14/5, to Eszter Farkas).

References

Astrup, J., Symon, L., Branston, N.M., Lassen, N.A., 1977. Cortical evoked potential and extracellular K+ and H+ at critical levels of brain ischemia. Stroke 8, 51–57.

Ay, H., Koroshetz, W.J., Vangel, M., Benner, T., Melinosky, C., Zhu, M., Menezes, N., Lopez, C.J., Sorensen, A.G., 2005. Conversion of ischemic brain tissue into infarction increases with age. Stroke 36, 2632–2636.

Ayata, C., 2013. Spreading depression and neurovascular coupling. Stroke 44 (6 Suppl 1), S87–S89.

Back, T., Ginsberg, M.D., Dietrich, W.D., Watson, B.D., 1996. Induction of spreading depression in the ischemic hemisphere following experimental middle cerebral artery occlusion: effect on infarct morphology. J. Cereb. Blood Flow Metab. 16, 202–213.

Bere, Z., Obrenovitch, T.P., Bari, F., Farkas, E., 2014a. Ischemia-induced depolarizations and associated hemodynamic responses in incomplete global forebrain ischemia in rats. Neuroscience 260, 217–226.

Bere, Z., Obrenovitch, T.P., Kozák, G., Bari, F., Farkas, E., 2014b. Imaging reveals the focal area of spreading depolarizations and a variety of hemodynamic responses in a rat microembolic stroke model. J. Cereb. Blood Flow Metab. 34, 1695–1705.

Chen, R.L., Balami, J.S., Esiri, M.M., Chen, L.K., Buchan, A.M., 2010. Ischemic stroke in the elderly: an overview of evidence. Nat. Rev. Neurol. 6, 256–265.

Claassen, J., Hirsch, L.J., Kreiter, K.T., Du, E.Y., Connolly, E.S., Emerson, R.G., Mayer, S.A., 2004. Quantitative continuous EEG for detecting delayed cerebral ischemia in patients with poor-grade subarachnoid hemorrh age. Clin. Neurophysiol 115, 2699–2710.

Clark, D., Institoris, A., Kozák, G., Bere, Z., Tuor, U., Farkas, E., Bari, F., 2014. Impact of aging on spreading depolarizations induced by focal brain ischemia in rats. Neurobiol. Aging 35, 2803–2811.

Dohmen, C., Sakowitz, O.W., Fabricius, M., Bosche, B., Reithmeier, T., Ernestus, R.I., Brinker, G., Dreier, J.P., Woitzik, J., Strong, A.J., Graf, R., Co-Operative Study of Brain Injury Depolarisations (COSBID), 2008. Spreading depolarizations occur in human ischemic stroke with high incidence. Ann. Neurol. 63, 720–728.

Dougherty, P.M., Li, Y.J., Lenz, F.A., Rowland, L., Mittman, S., 1997. Correlation of effects of general anesthetics on somatosensory neurons in the primate thalamus and cortical EEG power. J. Neurophysiol. 77, 1375–1392.

Dreier, J.P., 2011. The role of spreading depression, spreading depolarization and spreading ischemia in neurological disease. Nat. Med. 17, 439–447.

Dreier, J.P., Körner, K., Ebert, N., Görner, A., Rubin, I., Back, T., Lindauer, U., Wolf, T., Villringer, A., Einhäupl, K.M., Lauritzen, M., Dirnagl, U., 1998. Nitric oxide scavenging by hemoglobin or nitric oxide synthase inhibition by N-nitro-L-arginine induces cortical spreading ischemia when K+ is increased in the subarachnoid space. J. Cereb. Blood Flow Metab. 18, 978–990.

Dreier, J.P., Petzold, G., Tille, K., Lindauer, U., Arnold, G., Heinemann, U., Einhäupl, K.M., Dirnagl, U., 2001. Ischaemia triggered by spreading neuronal activation is inhibited by vasodilators in rats. J. Physiol. 531 (Pt 2), 515–526.

Dreier, J.P., Woitzik, J., Fabricius, M., Bhatia, R., Major, S., Drenckhahn, C., Lehmann, T.N., Sarrafzadeh, A., Willumsen, L., Hartings, J.A., Sakowitz, O.W., Seemann, J.H., Thieme, A., Lauritzen, M., Strong, A.J., 2006. Delayed ischaemic neurological deficits after subarachnoid haemorrhage are associated with clusters of spreading depolarizations. Brain 129 (Pt 12), 3224–3237.

Dugan, L.L., Choi, D.W., 1999. Hypoxia-ischemia and brain infarction. In: Siegel, G.J., Agranoff, B.W., Albers, R.W., Fisher, S.K., Uhler, M.D. (Eds.), Basic Neurochemistry: Molecular, Cellular and Medical Aspects. Lippincott-Raven, Philadelphia, pp. 711–730.

Duverger, D., MacKenzie, E.T., 1988. The quantification of cerebral infarction following focal ischemia in the rat: influence of strain, arterial pressure, blood glucose concentration, and age. J. Cereb. Blood Flow Metab. 8, 449–461.

Faber, J.E., Zhang, H., Lassance-Soares, R.M., Prabhakar, P., Najafi, A.H., Burnett, M.S., Epstein, S.E., 2011. Aging causes collateral rarefaction and increased severity of ischemic injury in multiple tissues. Arterioscler. Thromb. Vasc. Biol. 31, 1748–1756.

Farkas, E., Bari, F., 2014. Spreading depolarization in the ischemic brain: does aging have an impact? J. Gerontol. A Biol. Sci. Med. Sci. 69, 1363–1370.

Farkas, E., Luiten, P.G., 2001. Cerebral microvascular pathology in aging and Alzheimer's disease. Prog. Neurobiol. 64, 575–611.

Farkas, E., Obrenovitch, T.P., Institóris, Á., Bari, F., 2011. Effects of early aging and cerebral hypoperfusion on spreading depression in rats. Neurobiol. Aging 32, 1707–1715.
Fox, G., Gallacher, D., Shevde, S., Loftus, J., Swayne, G., 1993. Anatomic variation of the middle cerebral artery in the Sprague-Dawley rat. Stroke 24, 2087–2092 discussion 2092–3.
Hansen, A.J., Quistorff, B., Gjedde, A., 1980. Relationship between local changes in cortical blood flow and extracellular K+ during spreading depression. Acta Physiol. Scand. 109 (1), 1–6.
Hansen, A.J., Zeuthen, T., 1981. Extracellular ion concentrations during spreading depression and ischemia in the rat brain cortex. Acta Physiol. Scand. 113, 437–445.
Hartings, J.A., Watanabe, T., Bullock, M.R., Okonkwo, D.O., Fabricius, M., Woitzik, J., Dreier, J.P., Puccio, A., Shutter, L.A., Pahl, C., Strong, A.J., Co-Operative Study on Brain Injury Depolarizations, 2011. Spreading depolarizations have prolonged direct current shifts and are associated with poor outcome in brain trauma. Brain 134 (Pt 5), 1529–1540.
Hartings, J.A., Watanabe, T., Dreier, J.P., Major, S., Vendelbo, L., Fabricius, M., 2009. Recovery of slow potentials in AC-coupled electrocorticography: application to spreading depolarizations in rat and human cerebral cortex. J. Neurophysiol. 102, 2563–2575.
Hoffmann, U., Ayata, C., 2013. Neurovascular coupling during spreading depolarizations. Acta Neurochir Suppl. 115, 161–165.
Lapi, D., Colantuoni, A., 2015. Remodeling of cerebral microcirculation after ischemia-reperfusion. J. Vasc. Res. 52, 22–31.
Leão, A.A.P., 1944. Spreading depression of activity in the cerebral cortex. J. Neurophysiol. 7, 359–390.
Liao, L.D., Liu, Y.H., Lai, H.Y., Bandla, A., Shih, Y.Y., Chen, Y.Y., Thakor, N.V., 2015. Rescue of cortical neurovascular functions during the hyperacute phase of ischemia by peripheral sensory stimulation. Neurobiol. Dis. 75, 53–63.
Liu, F., McCullough, L.D., 2012. Interactions between age, sex, and hormones in experimental ischemic stroke. Neurochem. Int. 61, 1255–1265.
Liu, F., Yuan, R., Benashski, S.E., McCullough, L.D., 2009. Changes in experimental stroke outcome across the life span. J. Cereb. Blood Flow Metab. 29, 792–802.
Maslarova, A., Alam, M., Reiffurth, C., Lapilover, E., Gorji, A., Dreier, J.P., 2011. Chronically epileptic human and rat neocortex display a similar resistance against spreading depolarization in vitro. Stroke 42, 2917–2922.
Mayhan, W.G., Arrick, D.M., Sharpe, G.M., Sun, H., 2008. Age-related alterations in reactivity of cerebral arterioles: role of oxidative stress. Microcirculation 15, 225–236.
Nedergaard, M., 1996. Spreading depression as a contributor to ischemic brain damage. Adv. Neurol. 71, 75–83 discussion 83–4.
Park, L., Anrather, J., Girouard, H., Zhou, P., Iadecola, C., 2007. Nox2-derived reactive oxygen species mediate neurovascular dysregulation in the aging mouse brain. J. Cereb. Blood Flow Metab. 27, 1908–1918.
Popa-Wagner, A., Badan, I., Walker, L., Groppa, S., Patrana, N., Kessler, C., 2007. Accelerated infarct development, cytogenesis and apoptosis following transient cerebral ischemia in aged rats. Acta Neuropathol. 113, 277–293.
Rossi, D.J., Brady, J.D., Mohr, C., 2007. Astrocyte metabolism and signaling during brain ischemia. Nat. Neurosci. 10, 1377–1386.
Rubino, G.J., Young, W., 1988. Ischemic cortical lesions after permanent occlusion of individual middle cerebral artery branches in rats. Stroke 19, 870–877.
Obrenovitch, T.P., Chen, S., Farkas, E., 2009. Simultaneous, live imaging of cortical spreading depression and associated cerebral blood flow changes, by combining voltage-sensitive dye and laser speckle contrast methods. Neuroimage 45, 68–74.
Shin, H.K., Dunn, A.K., Jones, P.B., Boas, D.A., Moskowitz, M.A., Ayata, C., 2006. Vasoconstrictive neurovascular coupling during focal ischemic depolarizations. J. Cereb. Blood Flow Metab. 26, 1018–1030.
Somjen, G.G., 2001. Mechanisms of spreading depression and hypoxic spreading depression-like depolarization. Physiol. Rev. 81, 1065–1096.
Strong, A.J., Fabricius, M., Boutelle, M.G., Hibbins, S.J., Hopwood, S.E., Jones, R., Parkin, M.C., Lauritzen, M., 2002. Spreading and synchronous depressions of cortical activity in acutely injured human brain. Stroke 33, 2738–2743.
Ungvari, Z., Kaley, G., de Cabo, R., Sonntag, W.E., Csiszar, A., 2010. Mechanisms of vascular aging: new perspectives. J. Gerontol. A Biol. Sci. Med. Sci. 65, 1028–1041.
Warner, D.S., Sheng, H., Batinić-Haberle, I., 2004. Oxidants, antioxidants and the ischemic brain. J. Exp. Biol. 207 (Pt 18), 3221–3231.
Windmüller, O., Lindauer, U., Foddis, M., Einhäupl, K.M., Dirnagl, U., Heinemann, U., Dreier, J.P., 2005. Ion changes in spreading ischaemia induce rat middle cerebral artery constriction in the absence of NO. Brain 128, 2042–2051.
Woitzik, J., Hecht, N., Pinczolits, A., Sandow, N., Major, S., Winkler, M.K., Weber-Carstens, S., Dohmen, C., Graf, R., Strong, A.J., Dreier, J.P., Vajkoczy, P., COSBID study group, 2013. Propagation of cortical spreading depolarization in the human cortex after malignant stroke. Neurology 80, 1095–1102.